

**ME 461:
Finite Element
Analysis**

Spring | **2016**

The Development and Analysis of Helicopter Rotor Blades

Group Members:

Michael Roemer, Matthew Montana, Scott Novak, Mitchell Brush



PennState
College of Engineering

Table of Contents

Table of Contents	2
Executive Summary	3
Acknowledgements	4
List of Figures and Tables.....	5
Section 1: Background and Project Plan	6
Section 2: Development and Description of the CAD Geometry.....	7
Section 3: Development of Finite Element Meshes.....	10
Section 4: Development and Description of the Model Assembly and Boundary Conditions .	13
Section 5: Development and Description of Model Interactions	15
Section 6: Analysis of Finite Element Model.....	16
Section 7: Summary of Major Findings	17
Section 8: Works Cited.....	21

Executive Summary

This report summarizes the development and analysis of a helicopter rotor blade model using the finite element method. A CAD model of a Trex 600 RC helicopter blade was used for the analysis. Lift and drag forces were calculated and applied for simulation. ABAQUS finite element software was used as the primary medium of the simulation and analysis.

Initial research for the project involved a search for available CAD models of the desired blade, since blade geometry can be complex and SolidWorks development was not a project priority. With a fully developed and dimensioned model prepared for finite element analysis, research was performed to determine material properties in order to provide a realistic simulation.

The blade was subsequently imported into ANSYS for the meshing of complex geometries. Multiple iterations were required in order to obtain reasonable mesh quality. The meshed blade was then imported into ABAQUS, where material properties could be applied. With knowledge of the nominal operation conditions of the blade, reasonable load conditions were calculated and applied. A simple boundary condition was finally applied to constrain the model.

Finally, simulations were performed in order to study the effects of the loading conditions on the blade. Displacement, stress and strain visualizations were obtained and major results were able to be intuitively verified as a result of simple and expected behavior. Lastly, a frequency analysis was performed to study resonant frequency modes.

Acknowledgements

The team would like to thank Dr. Reuben Kraft for his guidance in major project decisions and for his persistence in instructing the finite element method and its applications.

List of Figures and Tables

- Figure 1:** Helicopter rotor visualization
- Figure 2:** Full view of blade in SolidWorks
- Figure 3:** Side views of blade in SolidWorks
- Figure 4:** Dimensioned drawing in SolidWorks
- Figure 5:** Full view of meshed blade
- Figure 6:** Free-end front and side views of meshed blade
- Figure 7:** Attached-end front and side views of meshed blade
- Figure 8:** Cut-view of mesh to show element quality
- Figure 9:** Boundary condition visualization
- Figure 10:** Distributed lift force loading condition
- Figure 11:** Distributed drag force loading condition
- Figure 12:** Analysis results – displacement, full blade view
- Figure 13:** Displacement along a path
- Figure 14:** Analysis results – stress distribution, full blade view
- Figure 15:** Analysis results – stress distribution, alternate view
- Figure 16:** Analysis results – strain distribution, full and zoomed blade views
- Figure 17:** Frequency analysis results
- Table 1:** Blade material properties
- Table 2:** Natural frequencies corresponding to the first 4 modes

Section 1: Background and Project Plan

Project Objective

Helicopter rotor blades are well-understood mechanical parts that are subject to common forces and stresses. These forces and stresses can be derived from well-defined relationships developed from decades of study on the helicopter (see Figure 1). As such, the team chose a rotor blade as the subject of study for this report. The overall purpose of this project is twofold – develop basic analysis of the rotor blade itself and detail the software steps used for the analysis. The finite element method (FEM) was used in conjunction with ABAQUS software for this report.

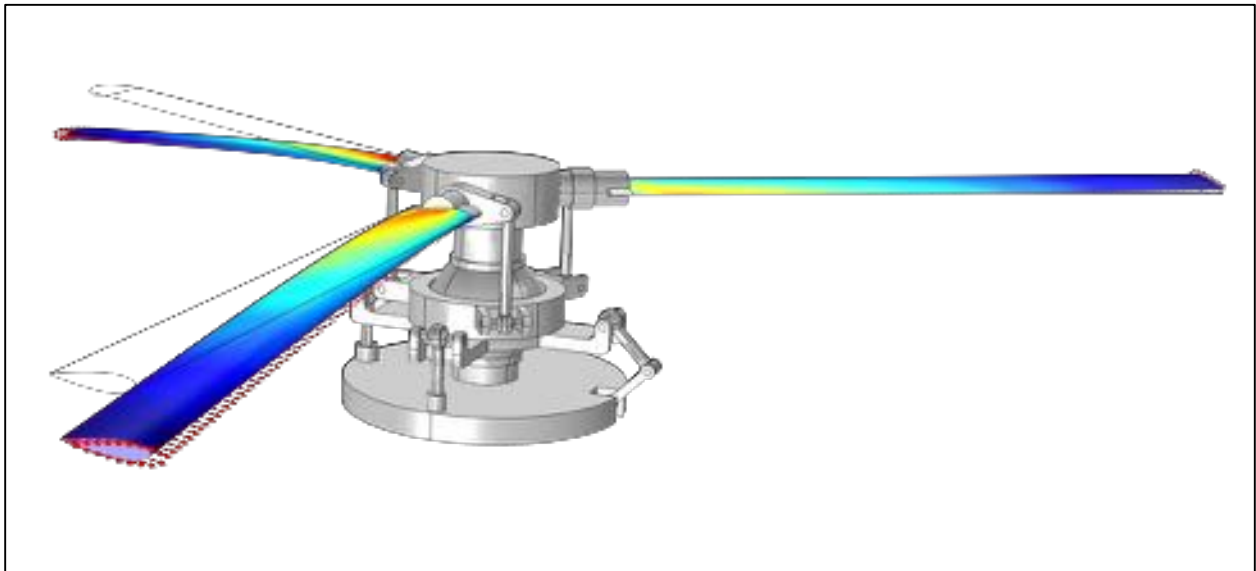


Figure 1: Schematic on stress distribution in rotor blades. Picture taken from comsol.pt.

Background Information

During use, helicopter rotors spin at well-defined rotational speeds that are throttled based on pilot commands. The rotors themselves are long airfoils designed to provide lift to the vehicle of attachment. This subjects them to drag and lift forces from the air as well as reaction forces that arise from connections to the main rotor. The magnitude of these forces are scaled depending on the size of the helicopter to be flown.

General Approach

For simplicity, the team will analyze the affect of wind (drag and lift forces) on a rotor blade. The blade in question is one from the Trex 600 RC helicopter, chosen because of the personal experience that one team member has with the product. A model for the blade was obtained and imported into ABAQUS for the definition of material properties, interactions, loads and boundary conditions before being meshed and simulated for results.

Section 2: Development and Description of the CAD Geometry

Before committing time to construct a blade fixture manually in SolidWorks, the team performed an external search for existing CAD files. A model of a Trex 600 main rotor blade was found [1] and chosen for this project since the group has access to a physical model of this RC helicopter. The model was then downloaded and imported into SolidWorks in order to create an engineering drawing in SI units, shown below.

Rendered images of the blade are shown below in Figures 2 and 3.

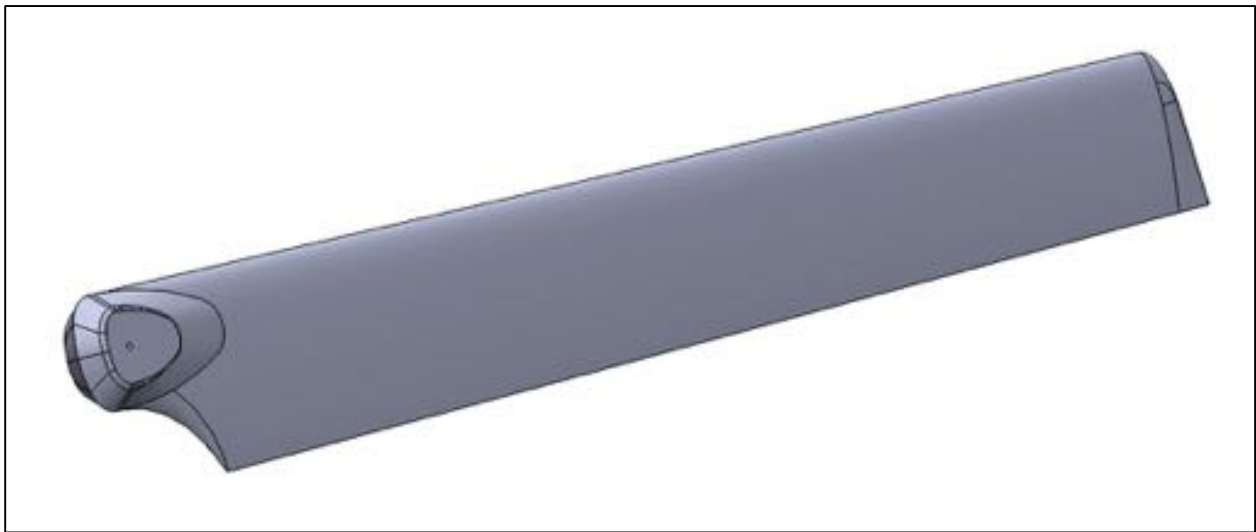


Figure 2: SolidWorks blade image - full view

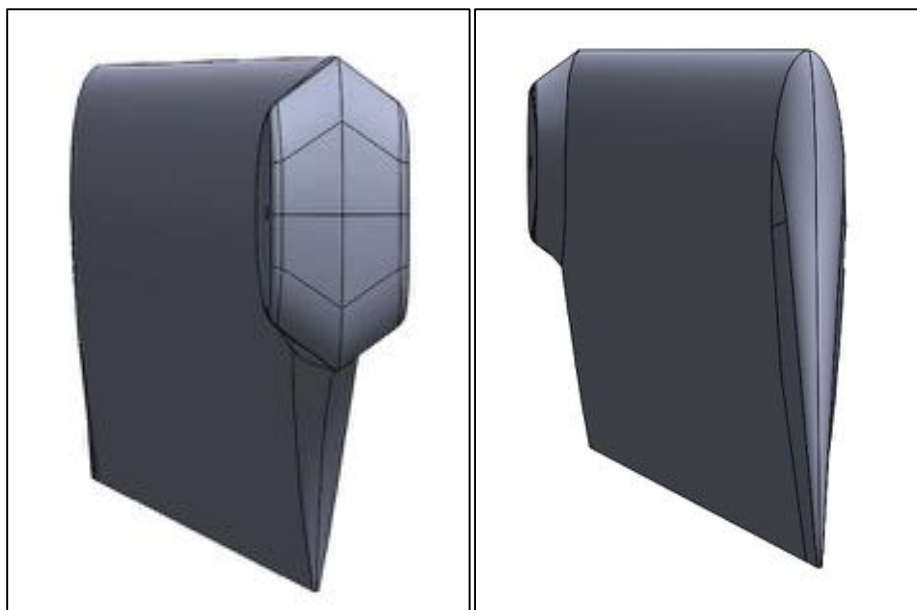


Figure 3: Solidworks blade images - side views

The SolidWorks engineering drawing of the blade is shown below in Figure 4.

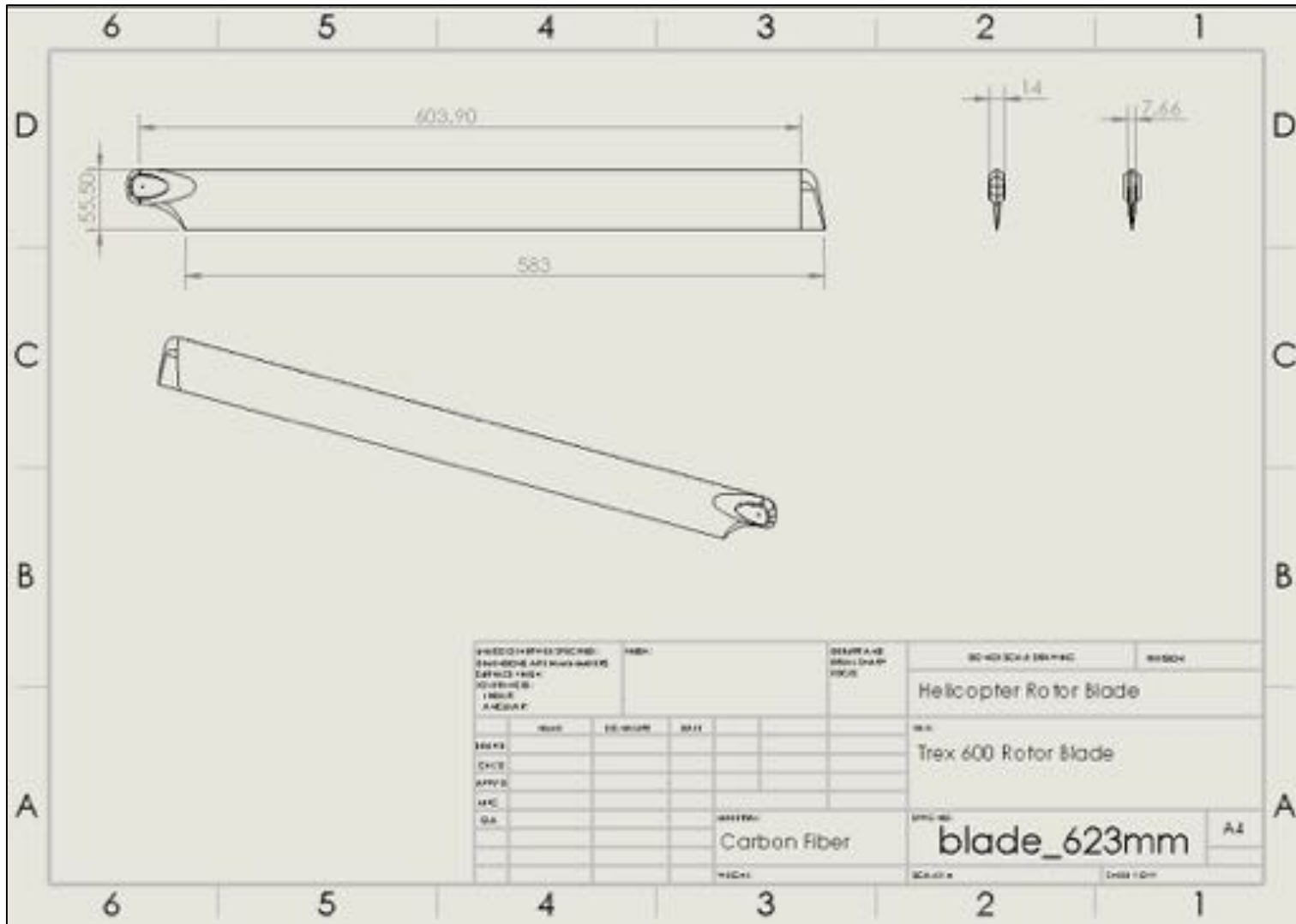


Figure 4: SolidWorks dimensioned drawing

Material Properties and External Loads

Further research suggested that most high-end Trex RC helicopters use carbon fiber for their blades, so this material was chosen. A tabulated list of material properties [2] is shown below in Table 1:

Table 1: Material properties

Property	Metric Value
<i>Tensile Strength</i>	3.53 GPa
<i>Young's Modulus</i>	230 GPa
<i>Density</i>	1.76 g/cm ³

The model helicopter carries a weight of approximately 3 kilograms or 6.7 pounds. This estimate was provided from a team member who owns a physical model of the Trex 600. Given that each blade needs to carry about half of the weight of the helicopter, each blade will need to produce a lift force of roughly **15 N** over its surface. This force will be distributed evenly across the low-pressure bottom surface of the blade that is used to provide lift to the machine.

To calculate the drag force on the blade, equation (1) below was used.

$$F_D = \frac{1}{2} * \rho * v^2 * C_D * A \quad (1)$$

The following parameters were used for this equation:

$$\rho = 1.204 \frac{kg}{m^3}$$

$$C_D = 0.04 [3]$$

$$v = 81.55 \frac{m}{s}$$

$$A = 0.623 m * 0.008 m = 0.005 m^2$$

The velocity, *v*, was calculated by taking the approximate rotational velocity of the blade during hover, 2500 rpm [5] converting it to radians per second and multiplying by the approximate distance to the center of gravity of the blade, or half its length. The area was calculated using dimensioned values. Using these parameters, the average drag force was calculated to be **0.812 N**. This force is to be distributed evenly across the area of the blade facing the direction of rotation of the blade.

Section 3: Development of Finite Element Meshes

To begin the process of creating a mesh for the rotor blade model described previously, the model was imported into a local SolidWorks license and re-saved as a *.step* format for ABAQUS compatibility. The model was then imported into ABAQUS with millimeters (mm) as the unit of distance.

A carbon fiber property was created using the property module in ABAQUS. Converting the previously defined units to match with the millimeter dimensions, the following properties were input for the material:

Young's Modulus: $210 * 10^3 \frac{N}{mm^2}$

Poisson's Ratio: 0.20 (for standard carbon fiber [4])

Density: $1.76 * 10^{-6} \frac{kg}{mm^3}$

No plastic deformation properties were defined for this model, as it is not expected to plastically deform. Given the complex geometry of the blade and its source, imprecise-geometry warnings were given by ABAQUS. It was subsequently discovered that no mesh types other than 3D stress tetrahedrals were feasible for the team to implement, given its limited ABAQUS experience. With the help of Dr. Kraft, the blade was exported into ANSYS 14.5, where its geometry was “healed” in order for a hex mesh to be made. The mesh in ANSYS was created with a scale factor of 10 and a minimum element size of 1.5. It was then exported back into ABAQUS, where the following images were grabbed from the screen. Figure 5 below is a full image of the resulting blade mesh.

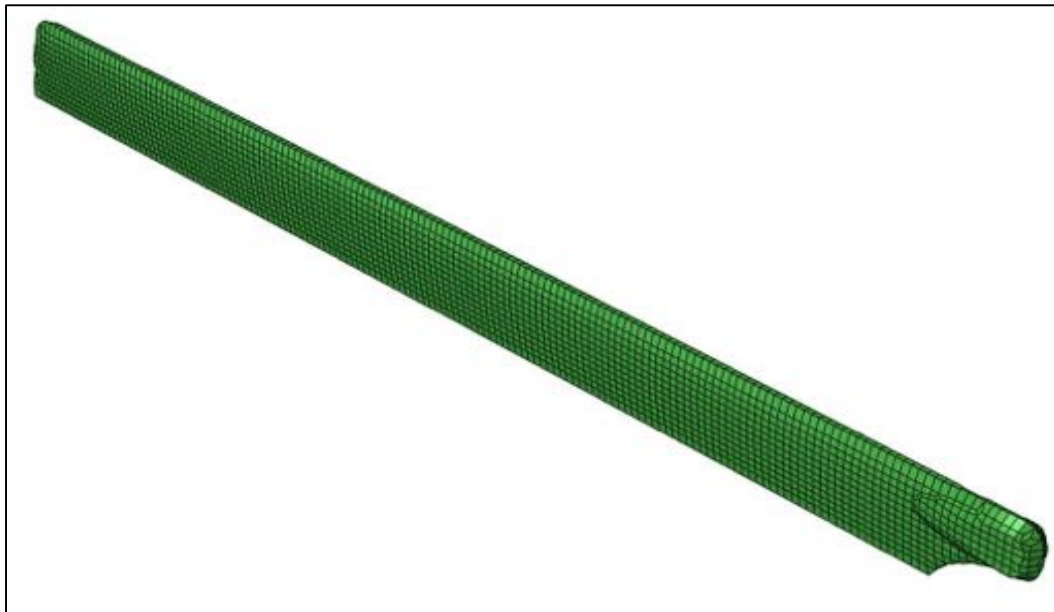


Figure 5: Mesh image - full view

Zoomed-in images of the free end of the blade are shown below in Figure 6.

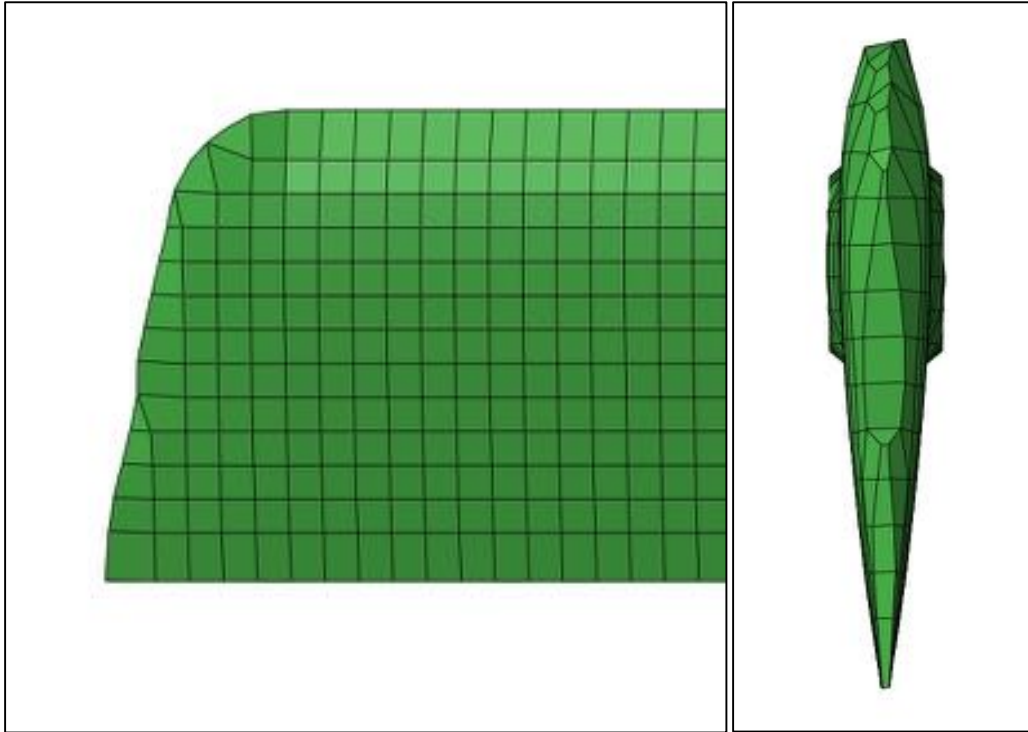


Figure 6: Mesh images - free end front and side views

Zoomed-in images of the end of the blade that connects to the rotor are shown below in Figure 7.

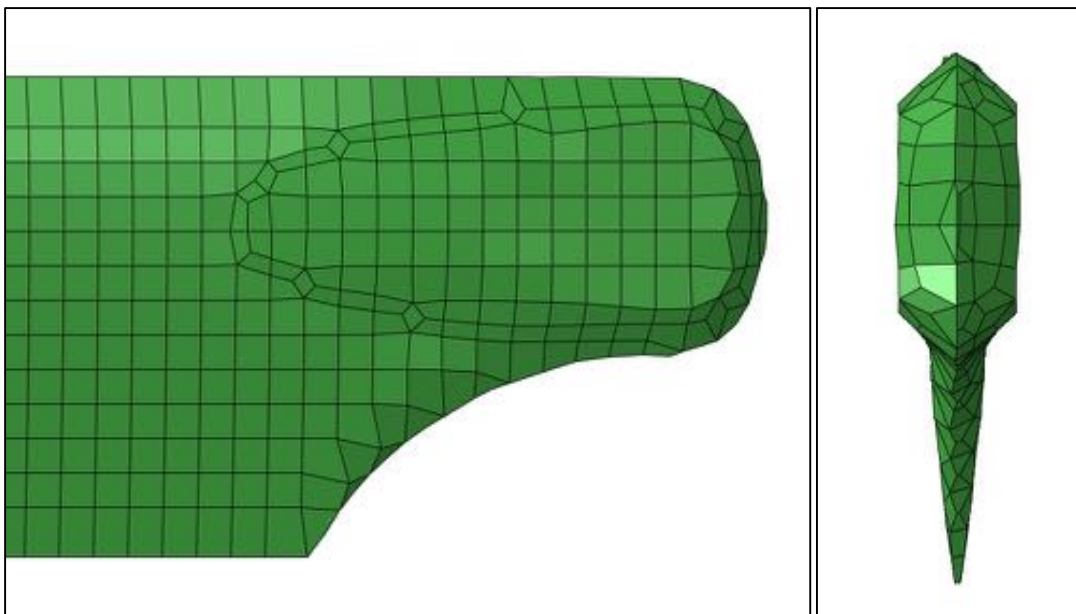


Figure 7: Mesh images - attached end front and side views

Finally, a cut plane was used to obtain an inner view of the mesh elements, shown below in Figure 8.

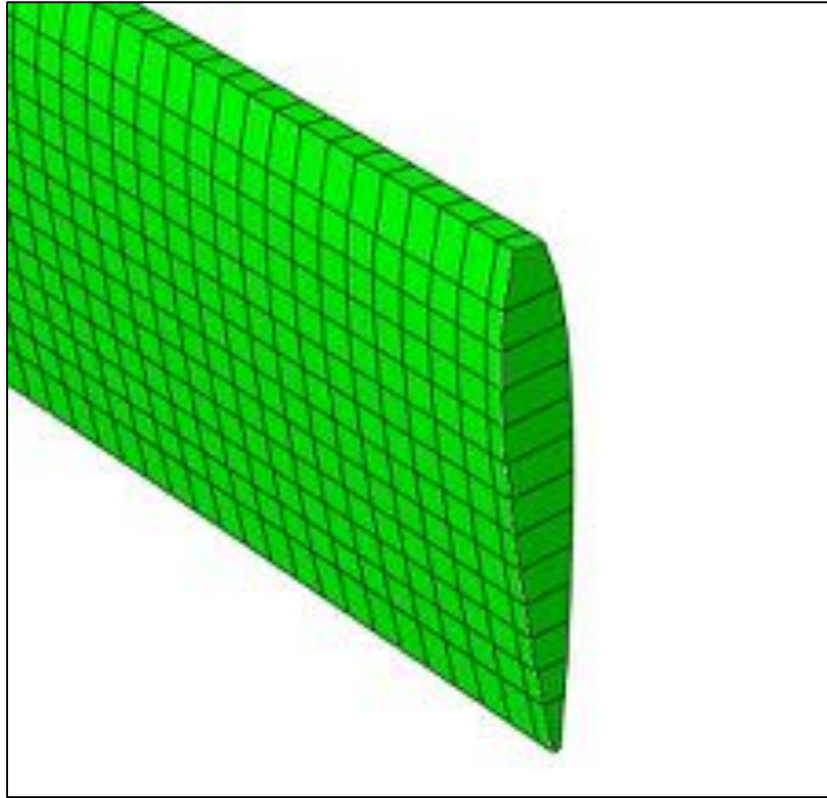


Figure 8: Cut-view of mesh showing element quality

Section 4: Development and Description of the Model Assembly and Boundary Conditions

In a preliminary attempt to simulate a load on the blade, boundary conditions were defined to fix the end of the blade that would generally be attached to a spinning rotor. Since the part was imported into ABAQUS as pre-meshed entity, it was more difficult than usual to define these constraints since nodes had to be selected instead of part faces. To begin, an encastre boundary condition was defined as shown below in Figure 8.

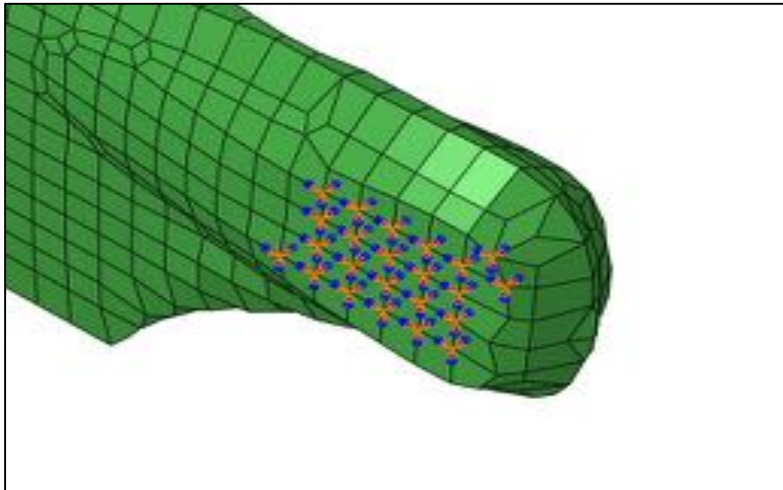


Figure 9: Encastre constraint boundary condition

The same boundary condition was applied to the opposite side of the blade to keep that end completely still. This was the only boundary condition applied in this preliminary simulation attempt. Next, a 15 N load was applied as a surface traction distributed across the bottom face of the blade as a lift force. The distribution of this applied load is shown below in Figure 9.

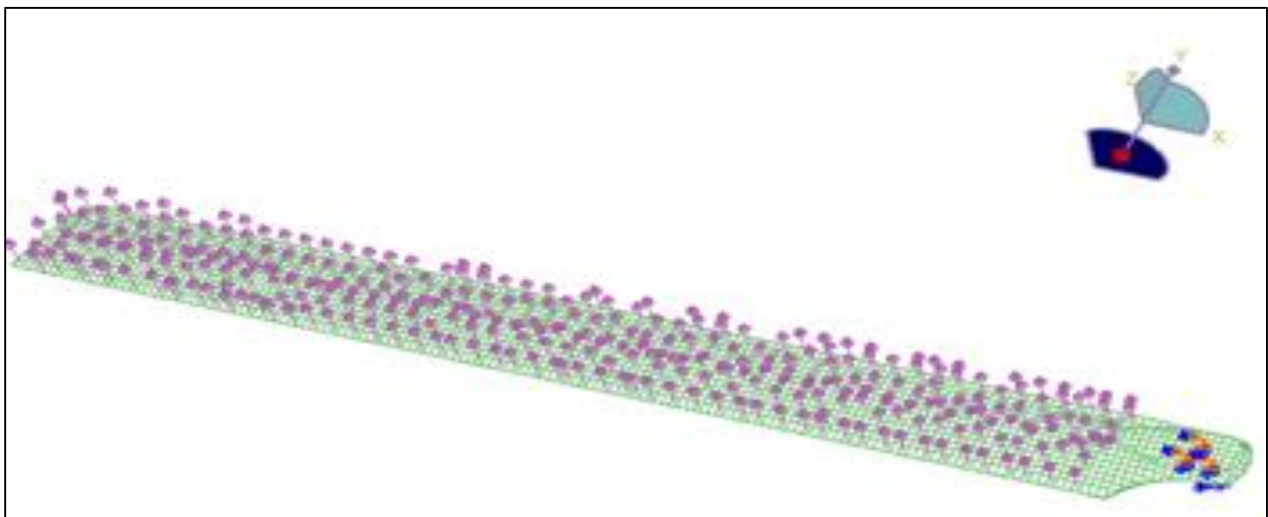


Figure 10: Distributed load on bottom face of blade. The vectors can be seen going up, simulating a lift force.

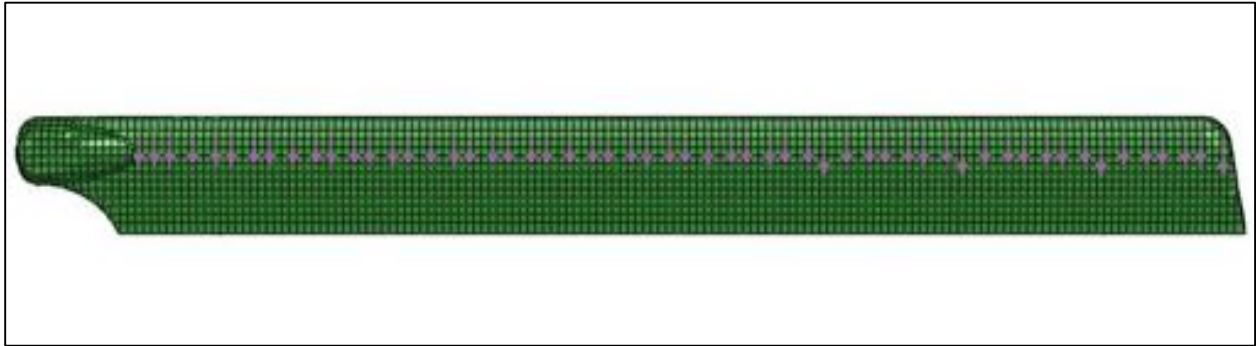


Figure 11: Distributed drag load on end of blade.

The calculated drag force of 0.812 N was subsequently applied head-on to the front of the blade, as shown above in Figure 10. This load was also applied as a distributed surface traction to the blade. Since the blade is designed to be aerodynamically-sound (low front-facing surface area), this relatively small load was not expected to have a significant impact on results.

Section 5: Development and Description of Model Interactions

For the entirety of this project, there was only the single blade in the model assembly. Furthermore, there was no expected plastic deformation in the blade. As a result, no interactions were defined for the simulations performed.

Section 6: Analysis of Finite Element Model

For the first simulation runs, a static general step was used for a step time of 0.1 seconds. Since the purpose was to initially show the effects of a constant load on the blade with no expected deformation and slow speeds, Abaqus/Standard was chosen over Abaqus/Explicit.

With the step, boundary condition and load fully defined, a job was created and ran. Given the chosen mesh size and quality created in ANSYS along with the simple load on the blade, the simulation ran in 24 seconds. PBS submission was not used for this reason. The preliminary results of the simulation are shown below.

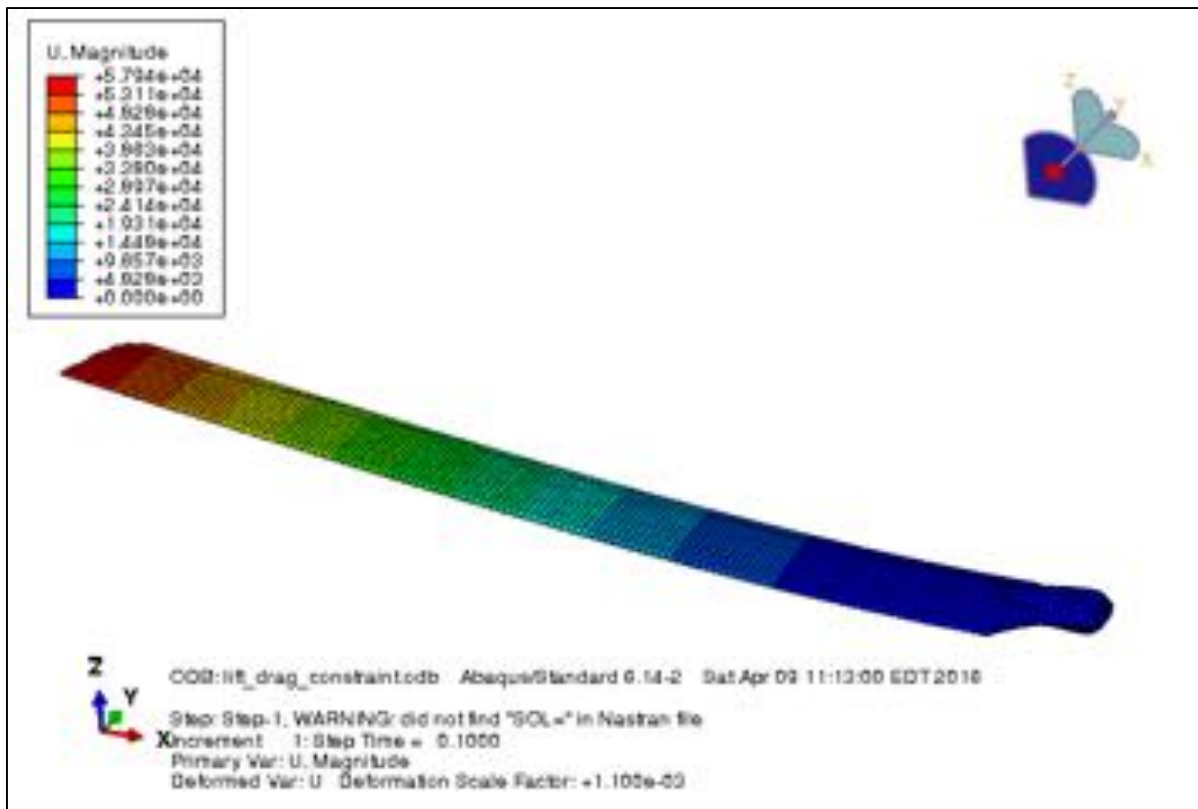


Figure 12: Displacement results on the blade. Max displacement was approximately 63.7 mm.

In order to obtain a better understanding of blade dynamics, simulations containing a frequency linear perturbation step were also performed. The first six natural frequencies of the blade were requested with a maximum frequency of 10,000 Hz to cap unnecessarily large frequency modes. The full results of both sets of simulations are detailed in the following section.

Section 7: Summary of Major Findings

With two sets of simulations, frequency and general-static, defined and run, data visualizations could then be used to validate data. Figure 12 showed maximum displacements that were slightly larger than expected but with a sensible distribution. To confirm this, a plot of displacement data was created on a path along the centerline of the blade, shown below in Figure 13.

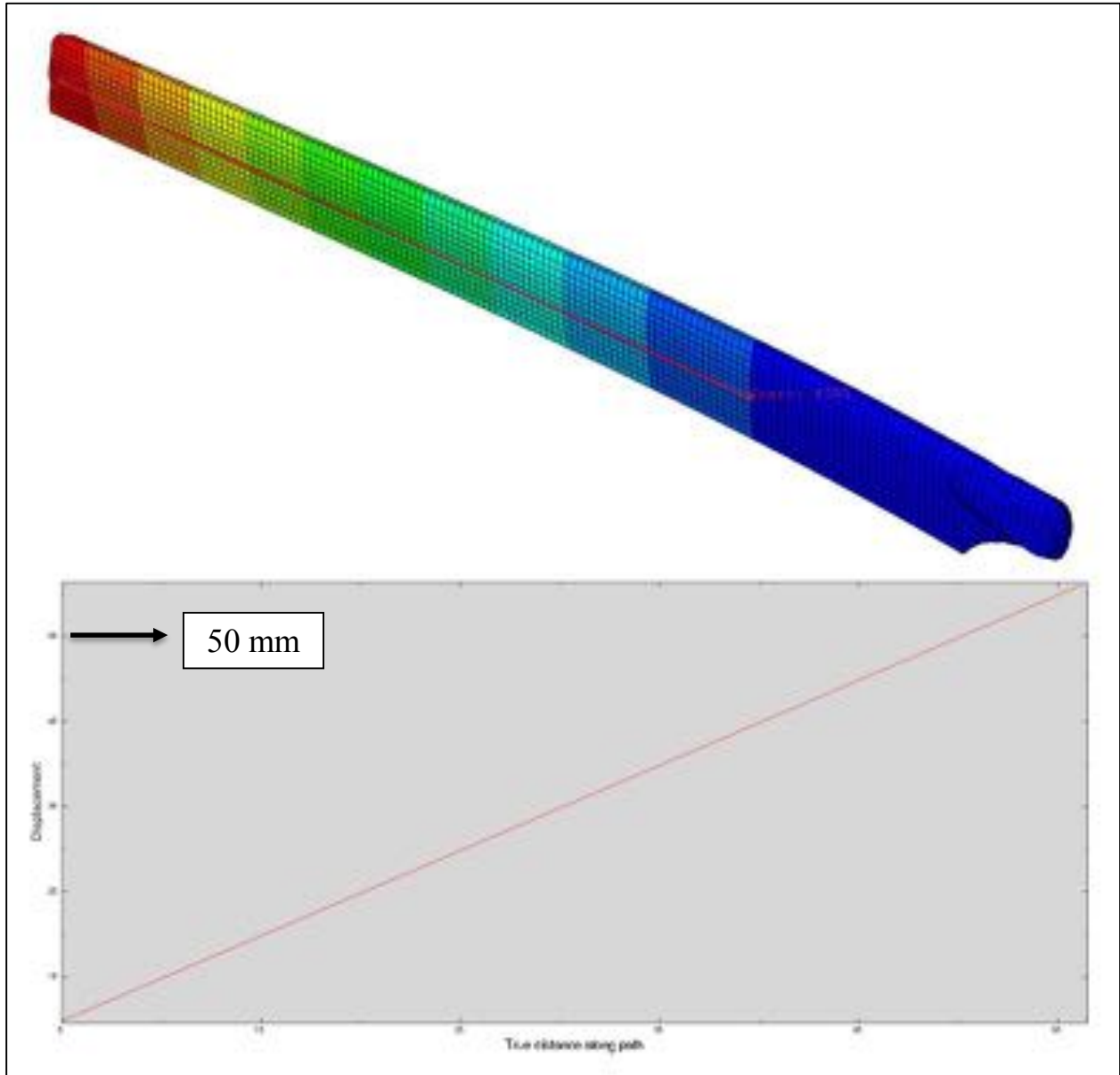


Figure 13: Defined path with displacement plot. For the bottom plot, both axes are dimensioned in millimeters.

Given the evenly-distributed lift force, a linear displacement curve along this path was expected. With only about 2.5 inches of displacement in the worst-case, the results seem consistent with reality as well.

Figures 14 and 15 show visualizations of the stress distribution of the blade under the defined nominal operating loads. Figure 15 in particular shows larger concentrations of stress around the corners of blade geometry. Refined mesh quality may have given better insight into the magnitudes of this stress, but limited experience with ANSYS prevented the team from making significant improvements to the mesh.

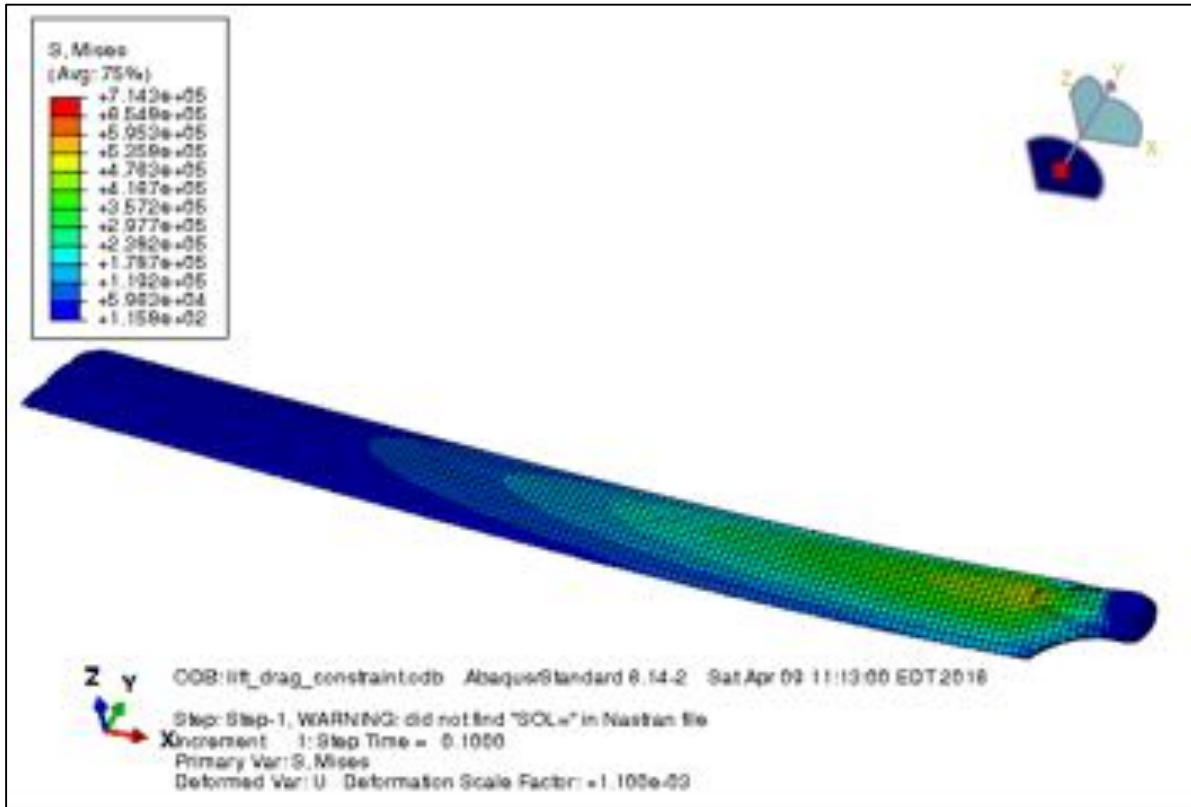


Figure 14: Stress distribution results

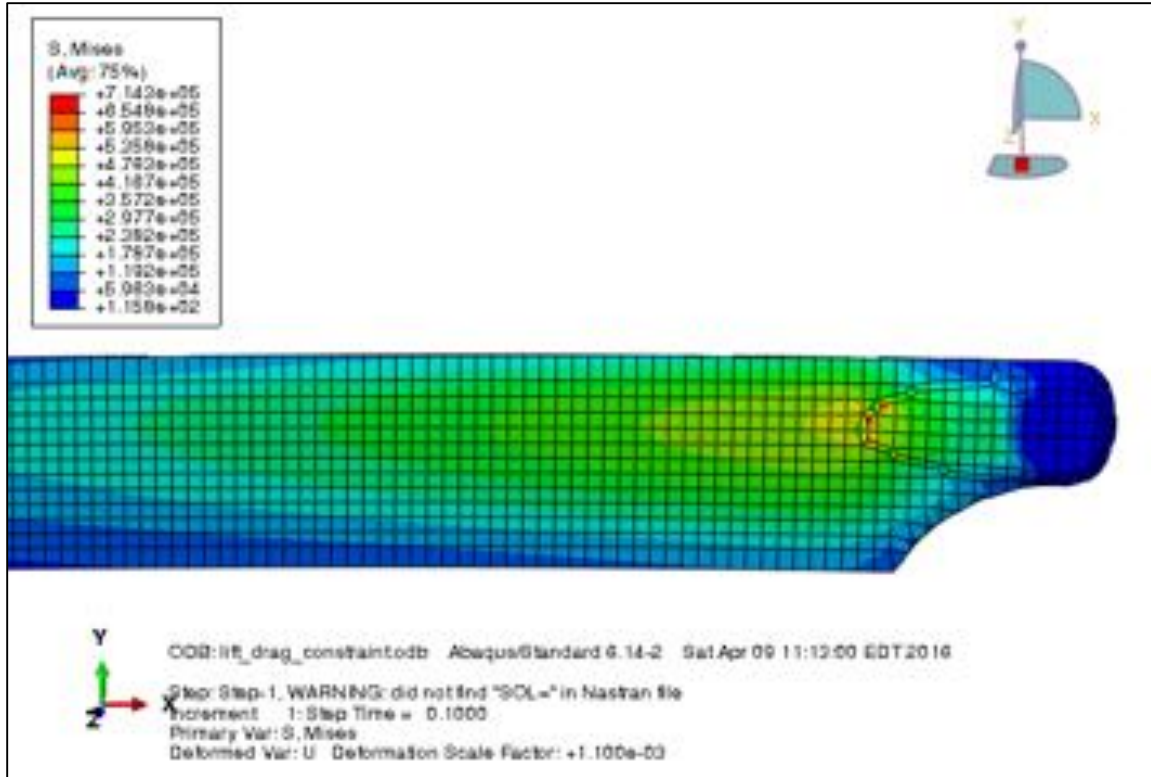


Figure 15: Alternate view of stress distribution

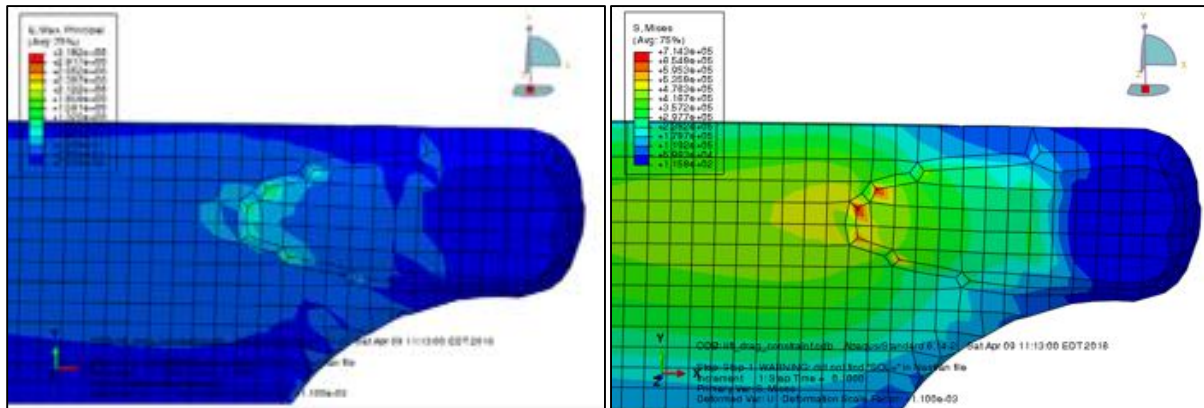


Figure 16: Strain distribution (left) and zoomed stress distribution (right)

Figure 16 shows the areas exposed to the highest magnitudes of stress and strain. This section of the beam was just outside the area that was constrained and is located on the edge of a small topology change in the blade. Therefore the stress concentrations expected in this region are sensible.

As described in the previous section, a frequency analysis was performed to uncover the primary modes of vibration present in this blade model. Although 6 natural frequencies were requested, only 4 are shown below.

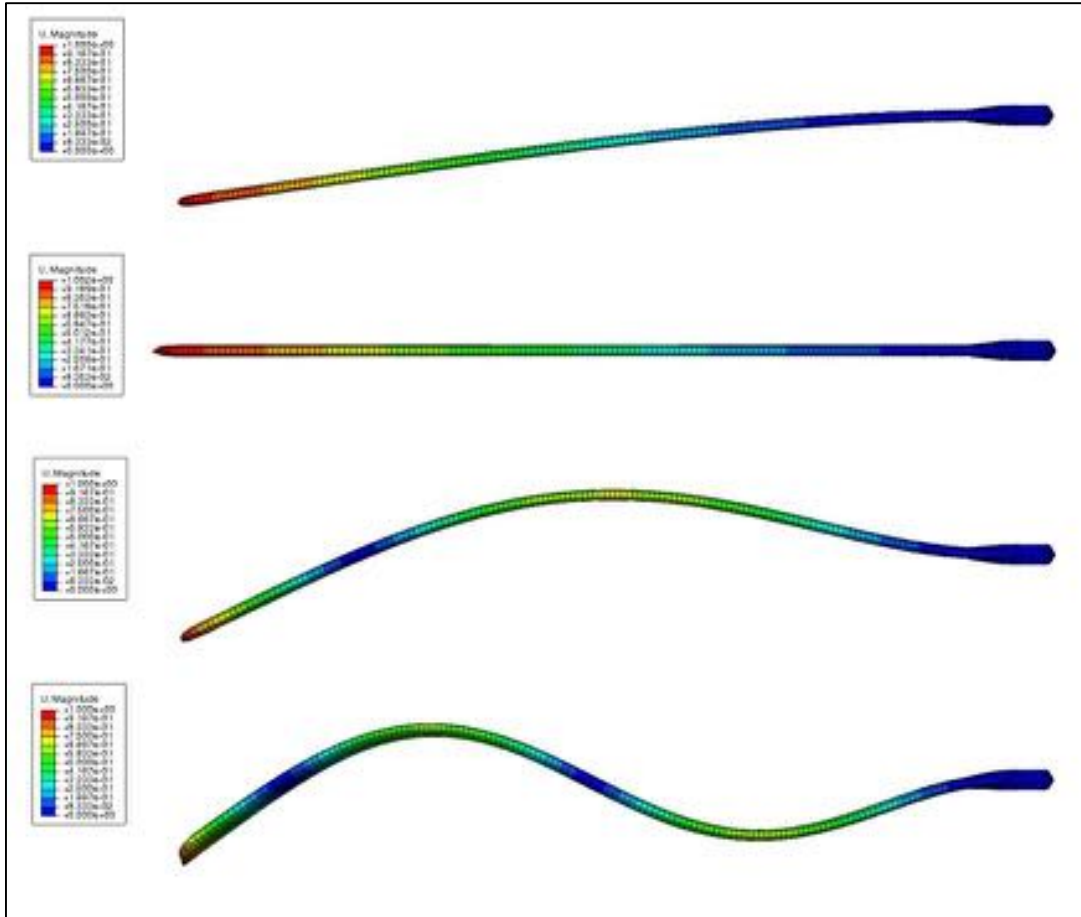


Figure 17: Blade natural frequencies 1-4, taken from a linear perturbation frequency step analysis.

Table 2 below details the specific frequencies for each mode.

Table 2: Frequencies corresponding to the first 4 modes

Frequency Analysis	
Mode Number	Natural Frequency (Hz)
1	1.0726
2	5.9954
3	6.6922
4	19.5790

Under the RC copter’s normal operating point, the blades should show very little vibration at constant operation. Given the high-stiffness material properties, any contact with projectiles should only cause very high frequency vibrations that are out of the range of these dominant modes. Therefore the team concluded that the blade will not be in danger of vibrating at a resonance frequency during the conditions described in this report.

Section 8: Works Cited

- [1] *Main Blade 623mm Edge*. N.p.: GrabCD, 3 Dec. 2013. 3DM.
- [2] "T300 Carbon Fiber Data Sheet." *Toryaca*. N.p., n.d. Web. 4 Feb. 2016.
- [3] "Drag Coefficient." *Wikipedia*. Wikimedia Foundation, n.d. Web. 04 Feb. 2016.
- [4] Sagala, Rickosnal. "Mechanical Properties of Carbon Fibre Composite Materials." *Mechanical Properties of Carbon Fibre Composite Materials*. N.p., n.d. Web. 24 Mar. 2016.
- [5] Abbeel, Pieter, and Adam Coates. "Autonomous Autorotation of an RC Helicopter." *Autonomous Autorotation of an RC Helicopter* (n.d.): n. pag. *Stanford.edu*. Web.